Nonlinear polarization rotation of elliptical light in cubic crystals, with application to cross-polarized wave generation

Aurélie Jullien

Laboratoire d'Optique Appliquée, Unité Mixte de Recherche 7639 CNRS, École Polytechnique, École Nationale Supérieure des Techniques Avancées, 91761 Palaiseau Cedex, France, and Thales Laser, RD 128, Domaine de Corbeville, 91400 Orsay, France

Olivier Albert, Gilles Chériaux, and Jean Etchepare

Laboratoire d'Optique Appliquée, Unité Mixte de Recherche 7639 CNRS, École Polytechnique, École Nationale Supérieure des Techniques Avancées, 91761 Palaiseau Cedex, France

Stoyan Kourtev, Nikolay Minkovski, and Solomon M. Saltiel

Faculty of Physics, University of Sofia, 5 J. Bourchier Boulevard, BG-1164, Sofia, Bulgaria

Received March 25, 2005; revised manuscript received June 24, 2005; accepted July 8, 2005

We have investigated theoretically and experimentally the nonlinear propagation of intense elliptically polarized light pulses along a fourfold axis of the cubic crystal BaF_2. Third-order nonlinear optical processes generate a cross-polarized wave, an effect that presents significant possibilities for application in femtosecond pulse contrast enhancement. The experimental setup consists of an input linear polarized light that passes through a cubic crystal sandwiched between two crossed quarter-wave plates. The exit orthogonal polarization-state production amount is measured at the output of an analyzer. When the light impinging on the sample is elliptically polarized with a quarter-wave plate at 22.5 deg, the achieved efficiency reaches 15%. It is more than twice that of a conventional polarization filter based on nonlinear ellipse rotation in an isotropic medium. This device is compared with previously reported polarization filtering [J. Opt. Soc. Am. B **21**, 1659 (2004)], in which a linearly polarized light produced a perpendicular field component. The theoretical model describes in detail the obtained dependencies and allows the different nonlinear processes that contribute to the generation of a cross-polarized wave to be distinguished. Possible applications are discussed.

OCIS codes: 190.0190, 190.3270, 190.4380, 190.4410, 190.4720, 230.5440.

1. INTRODUCTION

A lot of research has been devoted to nonlinear light propagation in various media. Nonlinear ellipse rotation (NER) has been studied in detail both experimentally and theoretically mostly in the case of isotropic media (Refs. 1 and 2 and references therein). This single-beam experimental arrangement has been used for the measurement of components of cubic susceptibilities[3,4] and applied for contrast-improvement purposes[5–8] and as a mode-locking device.[9] The system consists of a nonlinear material sandwiched between two crossed quarter-wave plates ($\lambda/4$). The amount of cross-polarized wave (XPW) generation is observed by the use of an output polarizer crossed with respect to the input polarization plane. The polarization-state optimal degree of ellipticity for the input beam, which maximizes the NER effect, is achieved when the axis of the $\lambda/4$ plate is rotated 22.5° with respect to the direction of input polarization.[10] Also, in a number of studies the effect of NER has been investigated by way of the propagation of a linearly polarized light in a birefringent medium. There, current applications are concerned with pulse reshaping,[10–12] nonlinear filtering and optical discrimination,[13] optical bistability,[14] and pulse cleaning.[15] In such a case the linearly polarized input light enters the crystal as an ordinary or extraordinary wave, and, as a result of the nonlinear effect, exchange of the energy occurs between the two polarization eigenstates.

In previous experiments[16,17] we have investigated a self-induced change of polarization state and XPW generation in the case of a linearly polarized light propagating along a fourfold axis in cubic and tetragonal crystals. In contrast to isotropic media, the third-order nonlinearity of cubic and tetragonal crystals possesses an anisotropy σ that generates an XPW signal that can exceed 10% in efficiency.

Here we extend our previous investigations on cubic crystals by using elliptically polarized light. It corresponds to a new configuration, to the author's knowledge, with respect to the above-mentioned studies[1,2] on NER processes that explored isotropic or birefringent media or both. This device will be called E-XPW (E for elliptical), and its properties will be compared with the L-XPW (L for linear) scheme we studied before.[16,17]

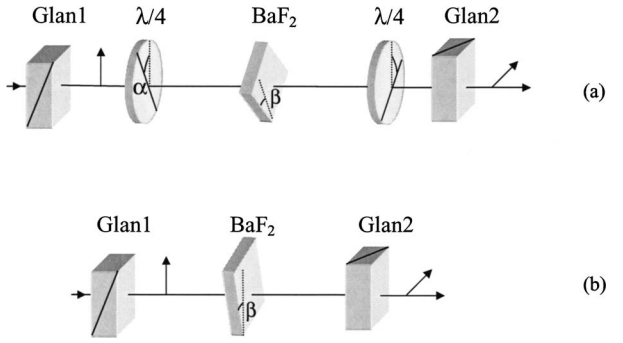

Fig. 1. Experimental arrangements for measuring XPW generation in a BaF_2 crystal. The input and output polarizers are crossed. (a) Scheme with elliptically polarized input light that involves two crossed λ/4 plates. (b) Scheme with linearly polarized input light without λ/4 plates. Angles α and β are defined on Fig. 2

A generalized theoretical model is also developed that enables predicting the processes that contribute to XPW generation in a nonlinear cubic (or tetragonal) system characterized by a third-order nonlinearity anisotropy σ and a light whose polarization can be either linear or elliptical. It gives evidence of the signal dependency on the orientation of the crystal with respect to the ellipse axis or the linearly polarized light direction, a fact that will dictate the setup characteristics. A study of these dependencies will allow a comparison of E-XPW and L-XPW efficiencies.

The setup for L-XPW and E-XPW generation in a cubic (BaF_2) crystal is shown in Fig. 1(a). It allows studying all possible configuration cases. It uses two polarizers and two λ/4 plates exactly crossed. When the input λ/4 plate is at $\alpha=0$ (α is the angle between the Y axis and the λ/4-plate fast axis), we recover the L-XPW setup as previously studied and shown for comparison on Fig. 1(b). When the input λ/4 plate is rotated by an angle α, then the second λ/4 plate is rotated at an angle $90°+\alpha$. This scheme allows suppression of the contribution from the unperturbed ellipse light to the E-XPW signal.

Filtering devices based on XPW generation are known to play an important role in current contrast improvements of femtosecond and ultraintense lasers. In such systems, the nonlinear process modifies mainly the polarization state of the ultrashort intense pulse, and the discrimination is obtained through the propagation along crossed polarizers. So, to compare the relative overall efficiencies from E-XPW and L-XPW devices, we have to consider not only the physical processes involved but also the extinction ratio of the respective setups. In the linear regime, the systems shown on Fig. 1(a) with $\alpha=22.5°$ and on Fig. 1(b) have contrast ratios of, respectively, 2.10^{-3} and 5×10^{-5}. The lower contrast for the E-XPW scheme is presumed to be due to the λ/4 plate's characteristics. A similar observation is reported in Ref. 5. We guess that the use of achromatic λ/4 plates should lead to improvement of their contrast ratio.[7]

2. THEORETICAL MODEL

We consider, in the slowly varying envelope approximation, plane-wave propagation equations in which an elliptically polarized light enters a cubic crystal along its fourfold z axis (see Fig. 2). Linear absorption and nonlinear absorption are neglected. By taking into account self-phase modulation, cross-phase modulation, and four-wave mixing processes, we obtain in the (fsz) frame the following system of equations:

$$\frac{dA}{dz}=i\gamma_1|A|^2A-i\gamma_2(|B|^2B-A^2B^*-2|A|^2B)+i\gamma_3(2|B|^2A+B^2A^*), \tag{1a}$$

$$\frac{dB}{dz}=i\gamma_1|B|^2B+i\gamma_2(|A|^2A-B^2A^*-2|B|^2A)+i\gamma_3(2|A|^2B+A^2B^*), \tag{1b}$$

where the two fields A and B are directed along fast (f) and slow (s) axes of the input λ/4 plate,

$$\gamma_1=\gamma_0\left[1-\frac{\sigma}{2}\sin^2(2\beta)\right],\quad \gamma_2=-\gamma_0\frac{\sigma}{4}\sin(4\beta),$$

$$\gamma_3=\gamma_0\left[\frac{\sigma}{2}\sin^2(2\beta)+\frac{1-\sigma}{3}\right],\quad \gamma_0=(6\pi/8\lambda n)\chi^{(3)}_{xxxx},$$

and $\sigma=(\chi^{(3)}_{xxxx}-2\chi^{(3)}_{xyyx}-\chi^{(3)}_{xxyy})/\chi^{(3)}_{xxxx}$ is the anisotropy of the $\chi^{(3)}$ tensor.[18,19] β is the angle of the crystallographic x axis of the crystal in the (xyz) frame with respect to the f direction, the direction of the A field. Equations (1a) and (1b) are totally symmetric with respect to the interchange of A and B (the difference in the sign in front of γ_2 is coming from the definition of the angle β). The terms with γ_1 correspond to self-phase modulation effects. The terms with γ_2 involve energy transfer from B to A components [Eq. (1a)] and from A to B components [Eq. (1b)]. The terms with γ_3 represent cross-phase modulation ($2|B|^2A$ and $2|A|^2B$) and four-wave mixing processes (B^2A^* and A^2B^*). We see the main difference between γ_2 terms and (γ_1 and γ_3) terms as a function of β for one full revolution of the crystal ($0\leqslant\beta\leqslant360$): The first ones have eight

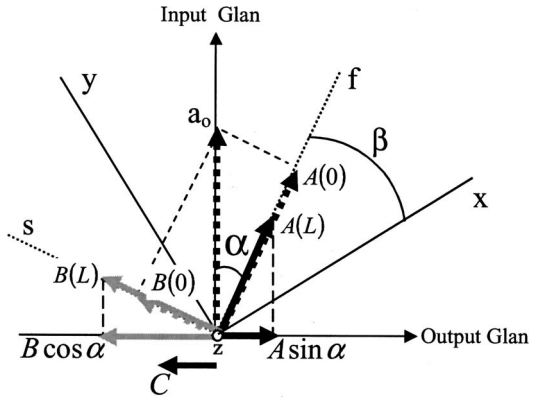

Fig. 2. Fields involved in the process and frames used in the model. The three frames are (a) input and output polarization directions, (b) f and s axes of the input $\gamma/4$ plate rotated at angle α with respect to frame a, (c) x and y crystallographic axes of the cubic crystal rotated at angle β with respect to frame b. The dashed thick arrows represent the input fields, and the solid thick arrows are output fields (see the text for further details).

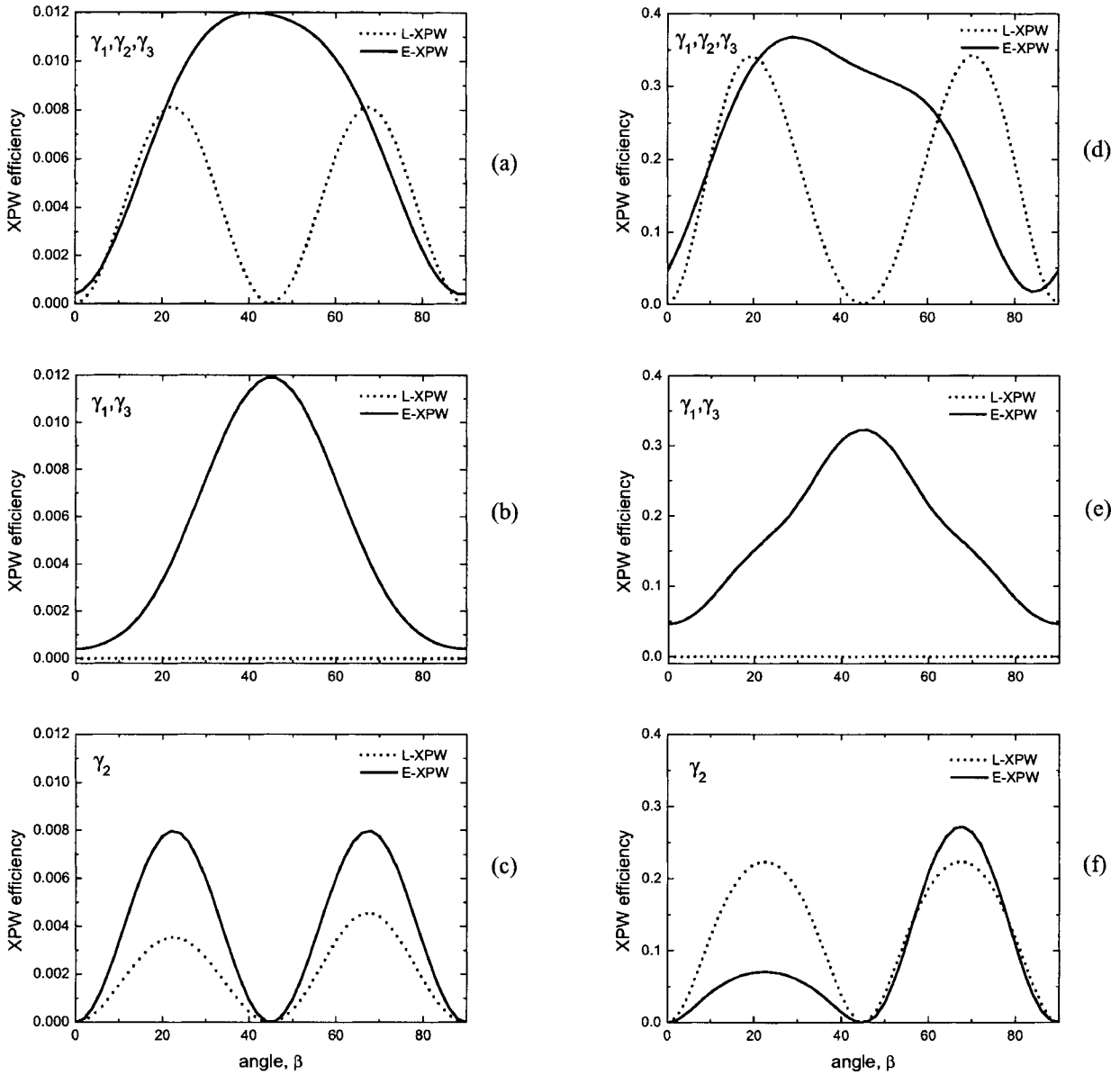

Fig. 3. Contribution of the different processes to the efficiency of the XPW generation obtained by numerical solution of system (1). (a)–(c) Low input intensity ($\gamma_0 a_0^2 L = 0.3$); (d)–(f) high input intensity ($\gamma_0 a_0^2 L = 2$).

maxima, whereas the second ones have four maxima.

As can be seen in system (1), the terms that reflect the possible phase mismatch and group-velocity mismatch are omitted, since cubic crystals such as BaF_2 have no birefringence, and consequently, the mismatch parameter $\Delta k = k_A - k_B = 0$, and the group-velocity dispersion parameter $\nu = 1/\nu_{g,A} - 1/\nu_{g,B} = 0$. Thus there is no modification of the polarization state of the input wave by linear effects.

Using system (1), one can model both processes, L-XPW and E-XPW. For linearly polarized input light the initial conditions are $A(0) = a_0$ and $B(0) = 0$. The resulting XPW intensity after the output polarizer is $(c\epsilon_0 n/2)|B(L)|^2$.

For the E-XPW process the elliptically polarized light input has two components shifted by a $\pi/2$ phase: $A(0) = a_0 \cos\alpha$ and $B(0) = ia_0 \sin\alpha$. At the output of the nonlinear crystal in the general case, both fields $A(L)$ and $B(L)$ are complex quantities. After the output polarizer, the XPW field is $C = A(L)\sin\alpha + iB(L)\cos\alpha$, and the intensity is $(c\epsilon_0 n/2)|C|^2$. Obviously, the XPW signal will be present only in the case of a nonlinear process acting between the two $\lambda/4$ plates.

A system of equations similar to Eqs. (1), but written for arbitrary orientation of the cubic crystal, has been solved numerically in the research of Hutchings *et al.*[20] for studying polarization instability and vector solitons in semiconductor waveguides. Here we investigate and solve numerically this system for the particular case of propagating all types of polarized light along a fourfold axis of a cubic crystal with the aim of investigating the optimal conditions for efficient XPW generation. The particular case of input linear polarization, namely, $\alpha = 0$, $B(z=0) = 0$, was previously solved analytically in the nondepleted regime.[17] Analysis of Eqs. (1) allows confirming that in this case the analytical model can be applied to the XPW generation when input intensities $\gamma_2 a_0^2 L < 1$, this value being the upper limit for which the use of the approxima-

tion for a nondepleted fundamental field is valid. Going from linear to elliptic light drastically changes the β-dependency characteristics. It turns out that in the linear polarization case γ_2 contributes mostly to the signal, although γ_1 and γ_3 are preponderant in the case of elliptically polarized input laser light.

To compare the role of the different processes (self-phase modulation, four-wave mixing, and cross-phase modulation), we plot in Fig. 3 some graphs of β dependence obtained by numerical solution of the system (1). We used two different values of the input intensity for the two kinds of scheme and for different terms included in the calculations [all γ's: Figs. 3(a) and 3(d); only γ_2: Figs. 3(c) and 3(f) and γ_1; γ_3: Figs. 3(b) and 3(e). It can be seen that at low intensity with all terms included [Fig. 3(a)] the pattern is an eightfold curve (over 360°) for L-XPW and a fourfold curve for E-XPW. At high intensity [Fig. 3(d)], symmetry breaking for elliptic light can be observed. It is the consequence from an interference of the A and B fields at the polarization plane of the output polarizer (see Fig. 2) and also a deviation from $(\sin 4\beta)^2$ dependence at high power. Indeed, if one solves the equation $dB/dz = -i\gamma_2(|B|^2 A)$, the result for the XPW intensity is $I_{XPW} \propto (\sin 4\beta)^2/(1+K\sin 4\beta)^2$, with $K=\gamma_2 a_0^2 L$. Some other examples of the numerical solution of Eqs. (1) are gathered on Figs. 4(c), 5(b), and 6(b), at precise values of $\gamma_2 a_0^2 L$ and σ.

The case of input circularly polarized light is realized for $\alpha = 45°$. This type of polarized light does not change its polarization properties and, consequently, cannot produce XPW for any input power and for any value of β.

3. EXPERIMENT AND DISCUSSIONS

The experiments have been performed using a single beam that propagates along the z axis of a [001]-cut barium fluoride (BaF_2) crystal. The sample used was 2 mm long, and its faces were uncoated. Two laser sources have been used: a colliding-pulse mode-locked dye laser (oscillator plus four-stage amplification, using maximum energy of 60 μJ and with duration 100 fs, frequency 10 Hz, and wavelength 620 nm) and a Ti:sapphire laser (oscillator plus chirped pulse amplification, using energy of 1.2 mJ and with duration 45 fs, frequency 1 kHz, and wavelength 800 nm). In most of the experiments the laser beam was focused on the sample with a 30 cm focal-length lens. The signals from two photodiodes, which measure input and output energies, are connected to a computer for signal averaging and processing.

Experimental results are presented as follows. In Subsection 3.A we present measurements of the intensity-induced rotation of the ellipse axes, which is the basic NER process. Then in Subsection 3.B we compare XPW efficiencies as a function of the β value for different ellipticities. In Subsection 3.C the disturbing role of self-phase modulation is pointed out through the analysis of the pulses spectrum.

A. Nonlinear Ellipse Rotation

We first analyze the influence of the ellipticity on the effect of nonlinear ellipse rotation. The input $\lambda/4$ plate [see Fig. 4(a)] is rotated at an angle α with respect to Y. Tuning the output Glan to reach the minimum of transmission is the simplest way of measuring the induced nonlinear rotation of the input elliptically polarized light.[16] At low intensity, we recover the position of the main ellipse axis at angle α—the angle that has been given to the input $\lambda/4$ plate rotation. At higher intensity the effect of NER is clearly observed. The amount of NER depends on both angles α and β. At power levels available for the experiment, $\alpha = 22.5°$ was the optimal angle for obtaining maximum NER. This value corresponds to the highest possible ellipticity from an initial linearly polarized light.

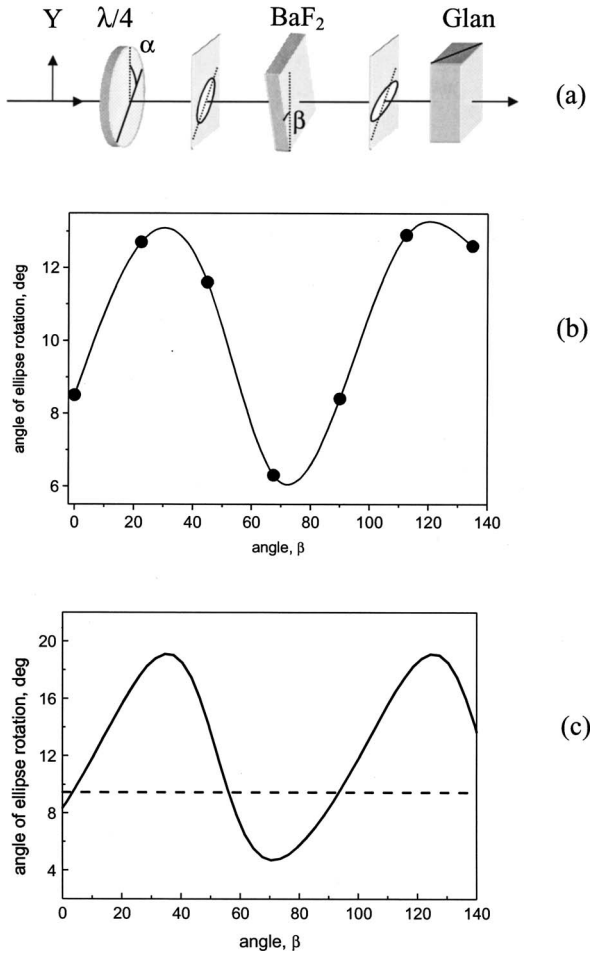

Fig. 4. (a) Experimental setup for measuring nonlinear ellipse rotation. (b) Variation of the measured rotation of the main ellipse axis as a function of sample rotation around its [001] axis. Input pulse energy is 12.5 μJ. The input $\lambda/4$ plate is rotated at $\alpha = 22.5°$. The curve is a guide for the eye. (c) Theoretical prediction for the ellipse rotation as obtained by numerical solution of system (1) for normalized intensity level $\gamma_0 a_0^2 L = 0.7$ and $\sigma = -1.2$. The dashed line is the amount of nonlinear ellipse rotation for isotropic media with $\sigma = 0$.

We analyzed the rotation of the main ellipse axis as a function of β with $\alpha = 22.5°$ and input energy of $U = 12.5$ μJ by using the colliding-pulse mode-locked laser. The experimental results are shown on Fig. 4(b). Figure 4(c) corresponds to the theoretical prediction obtained with the model, for a normalized intensity $\gamma_0 a_0^2 L = 0.7$. The anisotropy of the third-order nonlinearity is taken to be $\sigma = -1.2$. It is demonstrated that the nonlinear ellipse rotation is a periodic function of the angle β and reaches a

maximum rotation equal to 13°, counted from the input main axis position (22.5°). We note that the theoretical curve correctly describes the periodicity and the position of the maxima. However, the theoretically predicted amount of rotation exceeds the experimental one owing to the use of the plane-wave approximation. The dashed line illustrates the amount of nonlinear ellipse rotation from the isotropic media ($\sigma=0$). The obtained magnitude of nonlinear ellipse rotation is compatible with previously reported ones in isotropic media.[4]

B. Cross-Polarized Wave Generation as a Function of α and β

To compare the use of a linear or an elliptic input polarization for XPW generation, we performed transmission measurements of the signal coming out from the analyzer (Glan2) as a function of β for different α values. For the case $\alpha=0°$, the angle β is counted from the input polarization.

The results of the measurements of the XPW efficiency as a function of angle β using the setup shown on Fig. 1(a) are shown on Fig. 5(a) for three angles α of the $\lambda/4$ axis ($\alpha=0°$, 18°, and 22.5°). One can note two periodical behaviors with respect to β: $\pi/4$ periodicity for the L-XPW scheme ($\alpha=0°$) and $\pi/2$ periodicity for the E-XPW scheme ($\alpha\neq 0°$). This periodicity confirms that XPW generation using linear polarization depends only on γ_2 terms and indicates that in the elliptic polarization case γ_1 and γ_3 terms play the important role. The input energy for these measurements was 12.5 μJ, and the XPW generation efficiency was close to 8%. Theoretical curves are shown on Fig. 5(b). The theoretical patterns encountered for these two α angles are similar to the experimental ones. This agreement gives confidence for the correctness of the model. On Fig. 5(b) the theoretical value of XPW generation for the setup of Fig. 1(a) where the sample is isotropic ($\sigma=0$) is shown with a dashed line for the same length and amount of third-order nonlinearity as the one used for BaF_2. The advantage for using cubic crystals instead of an isotropic medium is evident.

Relative efficiencies for XPW generation in cubic crystals from linear and elliptic light have been investigated with the two laser femtosecond sources at $\lambda=620$ nm and at $\lambda=800$ nm. The experimental results on β dependencies at high input energy level are shown on Fig. 5(a). A pronounced shift in the optimal angle β for the scheme using $\lambda/4$ plates is observed as a function of α angle value. This experimental result corroborates theoretical findings concerning opposite signs from processes governed by γ_2 as noticed in the theoretical part [Fig. 3(f)]. We show on Fig. 6(a) the dependence of the XPW efficiency as a function of input energy. The theoretical curves that are shown on Fig. 6(b) give good agreement. At high input energy the two schemes (L-XPW and E-XPW) give the same efficiency; at lower intensity the scheme with elliptically polarized input is more efficient. The measured efficiency of 11% shown on Fig. 6(a) can be corrected from Fresnel reflections at the surfaces, leading to 15% conversion efficiency of internal light. Here also the advantage of the use of a sample with anisotropic cubic nonlinearity ($\sigma\neq 0$) is observed.

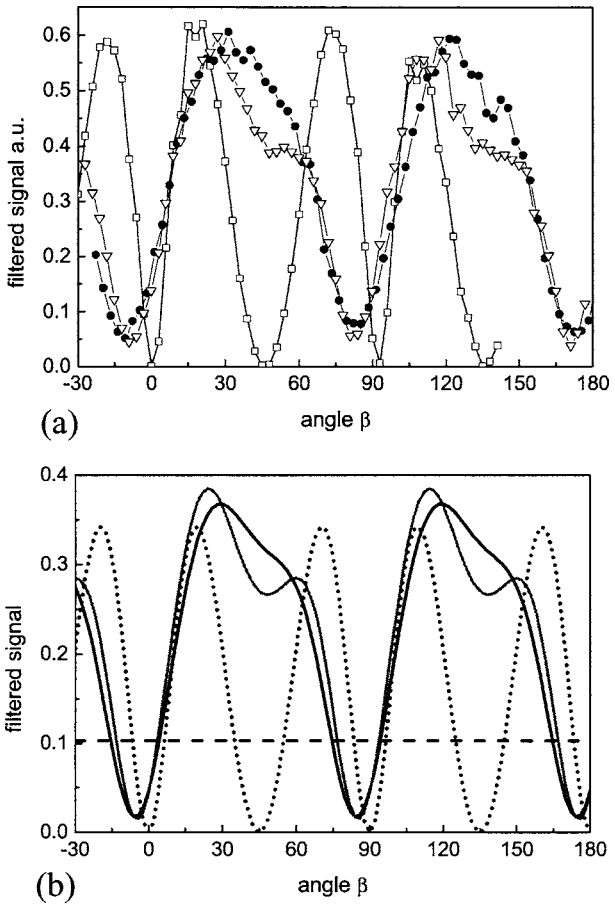

Fig. 5. (a) Variation of the experimentally measured XPW signal as a function of sample rotation around its [001] axis for a BaF_2 crystal for two different values of α for $\lambda/4$ plates. The input pulse energy is 12 μJ. Circles, $\alpha=22.5°$; triangles, $\alpha=18°$. The curves are corrected for imperfect crossing of the $\lambda/4$ plates. The curve with squares is obtained with the scheme without $\lambda/4$ plates [Fig. 1(b)]. (b) Theoretical prediction for the efficiency of the XPW generation as obtained by numerical solution of system (1) for normalized intensity level $\gamma_0 a_0^2 L=1.5$ and $\sigma=-1.2$. Dark curve, $\alpha=22.5°$; gray curve, $\alpha=18°$; dotted curve, $\alpha=0°$. The dashed line is the nonlinear ellipse rotation for the isotropic media with $\sigma=0$ when $\alpha=22.5°$.

We point out again that the difference in the theoretically predicted efficiency and the experimental one shown on Fig. 6 is the result of the use of the plane-wave approach in the theoretical model. Additionally, poorly defined spatial distribution does not allow us to calculate the relation between the energy of the pulses and the normalized input intensity $\gamma_0 a_0^2 L$.

Concluding this part, we note that, at the level of intensity used in these measurements, the optimal polarization ellipticity for maximum XPW generation is obtained for an angle $\alpha=22.5°$. The experimental curves are in good agreement with the theoretical predictions. The β behavior and the efficiency of E-XPW and L-XPW schemes have been compared. The overall transmission efficiency is quite equivalent for these two setups.

C. Self-Phase Modulation

The experiments described in the previous subsections have pointed out the crucial role of the anisotropy of the

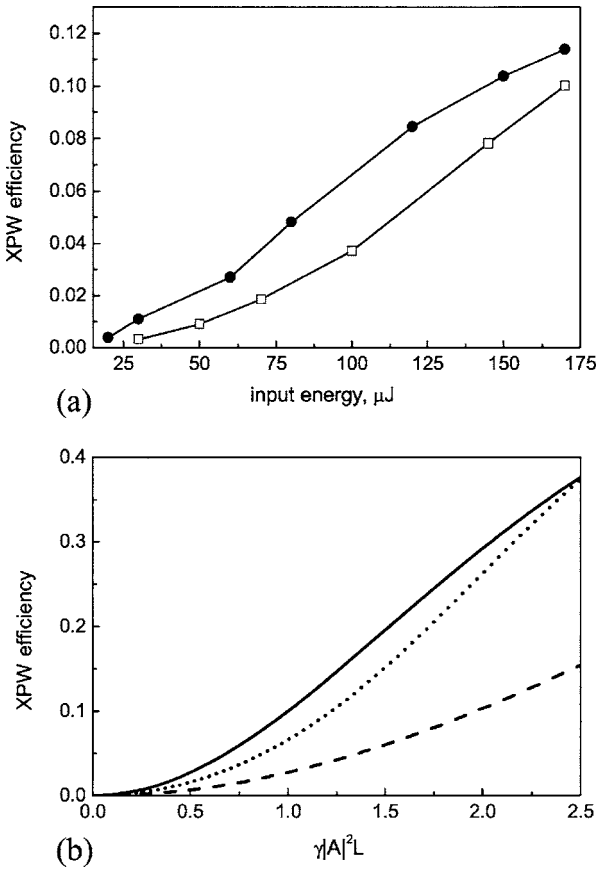

Fig. 6. (a) Variation of the measured XPW generation efficiency as a function of input energy for a BaF_2 crystal with the two schemes shown on Fig. 1: filled circles, E-XPW scheme [Fig. 1(a)]; open squares, L-XPW scheme [Fig. 1(b)]. Angle $\alpha=22.5°$ for the scheme on Fig. 1(a). In both measurements, the angle β is optimized for maximum efficiency. The curves are guides for the eye. (b) The respective theoretical predictions as obtained by numerical solution of system (1). Solid curve, E-XPW scheme [Fig. 1(a)]; dotted curve, L-XPW scheme [fig. 1(b)]. The dashed curve is the XPW generation efficiency for the scheme on Fig. 2(a) for isotropic media with $\sigma=0$.

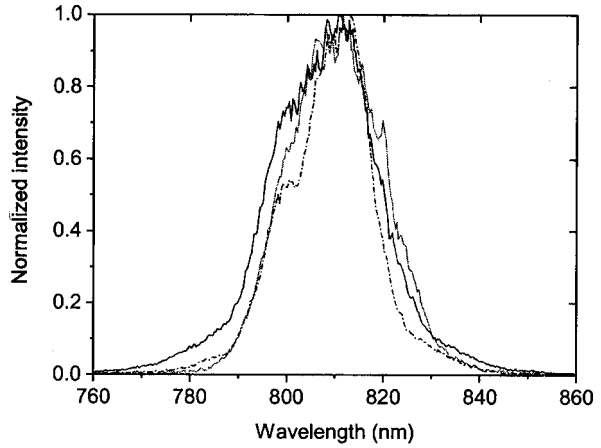

Fig. 7. Experimental spectra for XPW generation (10% efficiency) obtained by the L-XPW scheme (solid curve) and E-XPW scheme (dashed curve) compared with initial laser spectrum (gray curve).

third-order nonlinearity σ for XPW generation. We have observed that E-XPW generation is an interesting alternative to the L-XPW method, with equal transmission efficiency at high intensities. The drawback of the E-XPW technique would correspond to the fact that the process is then driven to some extent by both the self- and the cross-phase modulation (γ_1 and γ_3) terms.

At a high intensity level on the crystal, this leads to instability and modulations of the spatial and temporal characteristics. One can see the modulation of temporal characteristics by recording the resulting pulse spectrum, as we demonstrate with the $\lambda=800$ nm femtosecond laser. The pulse duration was about 45 fs. The input pulse energy was reduced to 100 μJ to avoid self-phase modulation due to focusing in the air, and the spectral behaviors of these two schemes were compared for various transmission efficiencies. Figure 7 compares spectra measured with E-XPW and L-XPW schemes with regard to the initial laser spectrum. These spectra were obtained in both cases with an XPW generation efficiency of 10%. The L-XPW spectrum is slightly shifted and presents a small broadening, but its shape remains mostly unmodified. On the other hand, the E-XPW spectrum presents some modulations and is clearly narrowed. As predicted by the theoretical model, the XPW process with elliptical input polarization is more sensitive to self-phase modulation. Self-phase modulation is usually the triggering effect of temporal prepulses or postpulses and phase distortions, which could be damaging to further utilization or amplification of the E-XPW pulse. This could be one of the limitations for the use of an elliptic light for contrast applications.

4. CONCLUSION

We have reported in detail theoretical and experimental investigations of nonlinear ellipse rotation and cross-polarized wave generation that occur when an intense elliptically polarized laser light wave propagates along the fourfold axis of a cubic crystal such as BaF_2. This scheme is a generalization from a previous arrangement that considered linearly polarized light and XPW generation. Drastic differences from these two configurations are observed as a function of the crystal orientation with respect to polarization direction. We have been able to differentiate the different physical processes that contribute mostly to the signal amplitude. In the case of linear polarization, creation of a XPW happens through the crystal nonlinear anisotropy. The case of elliptic light is more complex. The signal has a mixed contribution from rotation of the polarization and creation of a XPW. This last effect, which contains contributions of opposite signs, leads to a symmetry breaking of the signal as a function of the crystal orientation.

Efficient XPW generation can be the basis for a number of applications. One of them is the enhancement of the contrast of femtosecond pulses. As has been demonstrated by Jullien *et al.*[21] the XPW generation in the BaF_2 nonlinear filter can be used for four-order-of-magnitude improvement of the contrast of intense femtosecond pulses. It turns out that the use of an elliptic light can be an interesting alternative.

ACKNOWLEDGMENTS

The project was performed within the Access to Research Infrastructure contract (Light Matter Interaction: Nonlinear Processes and High Resolution Spectroscopy III, CT-1999-00086). N. Minkovski, S. Kourtev, and S. M. Saltiel thank the Laboratoire d'Optique Appliquée for the hospitality and support during their stay and also the Bulgarian Ministry of Science and Education for partial support with Science Fund grant 1201/2002. Corresponding author S. M. Saltiel can be reached by e-mail at saltiel@phys.uni-sofia.bg.

REFERENCES

1. G. P. Agrawal, *Nonlinear Fiber Optics* (U. of Rochester, 2001).
2. R. W. Boyd, *Nonlinear Optics* (Academic, 1992).
3. M. E. Orczyk, M. Samoc, J. Swiatkiewicz, and P. N. Prasad, "Dynamics of third-order nonlinearity of canthaxanthin carotenoid by the optically heterodyned phase-tuned femtosecond optical Kerr gate," J. Chem. Phys. **98**, 2524–2533 (1983).
4. M. Lefkir and G. Rivoire, "Influence of transverse effects on measurement of third-order nonlinear susceptibility by self-induced polarization state changes," J. Opt. Soc. Am. B **14**, 2856–2864 (1997).
5. D. Homoelle, A. L. Gaeta, V. Yanovsky, and G. Mourou, "Pulse contrast enhancement of high-energy pulses by use of a gas-filled hollow waveguide," Opt. Lett. **27**, 1646–1648 (2002).
6. A. Jullien, F. Auge-Rochereau, G. Cheriaux, J. P. Chambaret, P. d'Oliveira, T. Auguste, and F. Falcoz, "High-efficiency, simple setup for pulse cleaning at the millijoule level by nonlinear induced birefringence," Opt. Lett. **29**, 2184–2186 (2004).
7. M. P. Kalashnikov, E. Risse, H. Schönnagel, A. Husakou, J. Herrmann, and W. Sandner, "Characterization of a nonlinear filter for the front-end of a high contrast double-CPA Ti:sapphire laser," Opt. Express **12**, 5088–5097 (2004).
8. K. Sala and M. C. Richardson, "A passive nonresonant technique for pulse contrast enhancement and gain isolation," J. Appl. Phys. **49**, 2268–2276 (1978).
9. K. Sala, M. Richardson, and N. Isenor, "Passive mode locking of lasers with the optical Kerr effect modulator," IEEE J. Quantum Electron. **QE-13**, 915–924 (1977).
10. R. H. Stolen, I. Botineau, and A. Ashkin, "Intensity discrimination of optical pulses with birefringent fibers," Opt. Lett. **7**, 512–514 (1982).
11. B. Nikolaus, D. Grischkowsky, and A. C. Balant, "Optical pulse reshaping based on the nonlinear birefringence of single-mode optical fibers," Opt. Lett. **8**, 189–191 (1983).
12. H. G. Winful, "Self-induced polarization changes in birefringent optical fibers," Appl. Phys. Lett. **47**, 213–215 (1985).
13. M. Horowitz and Y. Silberberg, "Nonlinear filtering by use of intensity-dependent polarization rotation in birefringent fibers," Opt. Lett. **22**, 1760–1763 (1997).
14. K. Otsuka, J. Yumoto, and J. J. Song, "Optical bistability based on self-induced polarization-state change in anisotropic Kerr-like media," Opt. Lett. **10**, 508–510 (1985).
15. J. L. Tapie and G. Mourou, "Shaping of clean, femtosecond pulses at 1.053 μm for chirped-pulse amplification," Opt. Lett. **17**, 136–138 (1992).
16. N. Minkovski, S. M. Saltiel, G. I. Petrov, O. Albert, and J. Etchepare, "Polarization rotation induced by cascaded third-order processes," Opt. Lett. **27**, 2025–2027 (2002).
17. N. Minkovski, G. I. Petrov, S. M. Saltiel, O. Albert, and J. Etchepare, "Nonlinear polarization rotation and orthogonal polarization generation experienced in a single-beam configuration," J. Opt. Soc. Am. B **21**, 1659–1665 (2004).
18. W. A. Schroeder, D. S. McCallum, D. R. Harken, M. D. Dvorak, D. R. Andersen, A. L. Smirl, and B. S. Wherrett, "Intrinsic and induced anisotropy of nonlinear absorption and refraction in zinc blende semiconductors," J. Opt. Soc. Am. B **12**, 401–415 (1995).
19. M. D. Dvorak, W. A. Schroeder, D. R. Andersen, A. L. Smirl, and B. S. Wherrett, "Measurement of the anisotropy of two-photon absorption coefficients in zincblende semiconductors," IEEE J. Quantum Electron. **30**, 256–267 (1994).
20. D. C. Hutchings, J. S. Aitchison, and J. M. Arnold, "Nonlinear refractive coupling and vector solitons in anisotropic cubic media," J. Opt. Soc. Am. B **14**, 869–879 (1997).
21. A. Jullien, O. Albert, F. Burgy, G. Hamoniaux, J.-P. Rousseau, J.-P. Chambaret, F. Augé-Rochereau, G. Chériaux, J. Etchepare, N. Minkovski, and S. M. Saltiel, "10^{-10} temporal contrast for femtosecond ultraintense lasers by cross-polarized wave generation," Opt. Lett. **30**, 920–922 (2005).